Analyst

PAPER

View Article Online
View Journal | View Issue

Cite this: *Analyst*, 2015, **140**, 4224

An iridium oxide microelectrode for monitoring acute local pH changes of endothelial cells

Shu Rui Ng*[a,b] and Danny O'Hare[a]

Received 26th February 2015,
Accepted 13th April 2015

DOI: 10.1039/c5an00377f

www.rsc.org/analyst

pH sensors were fabricated by anodically electrodepositing iridium oxide films (AEIROFs) onto microelectrodes on chips and coated with poly(ethyleneimine) (PEI) for mechanical stability. These demonstrate super-Nernstian response to pH from pH 4.0 to 7.7 in chloride-free phosphate buffer. The surface of the chip was coated with fibronectin for the attachment of porcine aortic endothelial cells (PAECs). The working capability of the pH sensor for monitoring acute local pH changes was investigated by stimulating the PAECs with thrombin. Our results show that thrombin induced acute extracellular acidification of PAECs and dissolution of fibronectin, causing the local pH to decrease. The use of PD98059, a mitogen-activated protein kinase (MAPK) inhibitor, reduced extracellular acidification and an increase in local pH was observed. This study shows that our pH sensors can facilitate the investigation of acute cellular responses to stimulation by monitoring the real-time, local pH changes of cells attached to the sensors.

Introduction

The development of electrochemical microsensors for the study of cell metabolism is an interesting but challenging area of research.[1–4] The miniaturisation of sensors is advantageous in reducing the amount of costly biological reagents required due to the small sample volume of the chip. The sensing surface is on a similar length scale to the endothelial cells (ECs) (25 μm), allowing the sensor to be in close proximity to cells, thereby reducing diffusional distance, improving response time towards the target analyte and enabling the investigation of biological variability through parallel independent measurements taken from a small number of cells.[5] A significant problem with all biological measurements is to address the twin demands of maintaining a suitable healthy environment for the cells whilst ensuring that the sensor is able to function. Both sides of the interface – biocompatibility and sensor compatibility – need careful engineering to obtain meaningful results.[6,7] Cells are highly sensitive to their biochemical and biomechanical environment[8] and alterations to their environment can affect the responses of the cells which the researchers are attempting to measure. It is therefore challenging to interface cells with microsensors on a chip.

Firstly, adherent cells require a matrix to attach themselves onto the substrate to survive.[8] Secondly, the experiments need to be performed in cell culture medium to prevent unexpected or undetected changes in the cells due to a sudden change in the biochemical environment, such as when a buffer solution is used, for example phosphate buffer, it leads to losses of essential divalent cations due to the low solubility product. Thirdly, the adsorption of proteins from the cell culture medium and those secreted by the cells onto the electrodes causes the sensors to undergo biofouling and suffer reduced sensitivity.[9]

Despite the above challenges, our group is interested in developing electrochemical microsensors to study the acute metabolic and signaling responses of cells to various stimuli, such as growth factors. ECs are cells which line the blood vessels and are actively involved in angiogenesis, a process by which new blood vessels are formed from the pre-existing ones.[10] Understanding of EC metabolism and its intracellular pathways are essential for developing treatment of diseases such as cardiovascular disease and cancer which are associated with EC dysfunction, and pathological angiogenesis where the metabolism of ECs is altered.[11] EC metabolism is influenced by biochemical stimuli, such as pH, concentrations of dissolved O_2 and glucose, interactions with soluble factors and the extracellular matrix[12] and mechanical stimuli such as shear stress.[13] Alterations in the rate of EC metabolism in response to these stimuli occur through intracellular pathways which can manifest as changes in the concentrations of metabolic markers such as pH, lactate and CO_2.[12] The extracellular pH is a good indicator of EC metabolism since an increase in energy metabolism enhances glycolysis, which converts

[a]*Department of Bioengineering, Imperial College London, UK SW7 2AZ. E-mail: d.ohare@imperial.ac.uk; Fax: +44 (0)20 7594 5179; Tel: +44 (0)20 7594 5173*
[b]*School of Chemical and Biomedical Engineering, Division of Bioengineering, Nanyang Technological University, Singapore S637457. E-mail: shurui.ng@gmail.com; Tel: +65 68815381*

glucose to pyruvate in the cell. ECs mainly convert pyruvate to lactate even under physiological O_2 concentrations.[11] Lactate and H^+ are then transported out of the cells, leading to extracellular acidification.[14,15] As cells are only able to sense and respond to stimuli in their immediate surroundings,[16] it is more realistic to measure the local pH changes in the vicinity of the ECs instead of the bulk solution. The use of microelectrodes on a flat substrate for pH sensing is advantageous over high-resolution mobile pH sensors integrated with scanning electrochemical microscopy,[17] atomic force microscopy[18] or scanning ion conductance microscopy[19] since the cells can attach onto the electrode. This decreases the time taken by H^+ to diffuse into the electrode for the measurement of the local pH changes of the cells. Hence, our aim is to develop a potentiometric pH microsensor which can be applied to monitor and estimate the acute local pH changes of ECs cultured on it in cell culture medium and extend the range of analytes and of the chip-based devices that we have already shown as having demonstrable utility in early stage responses in angiogenesis[20,21] and host–pathogen interactions.[22] Notably, there is no commercially available pH sensor of similar size to the sensing elements in the array (25 μm diameter) reported here.

The measurement of pH is typically achieved using potentiometric pH sensors. However, the glass pH electrode has high impedance, suffers from slow response time, is mechanically fragile and not amenable to extreme miniaturisation.[23] In contrast, metal–metal oxide electrodes such as the antimony electrode,[24] iridium–iridium oxide (Ir–IrOx) film electrode,[25] gold–IrOx film microelectrode,[4,26–28] platinum–IrOx film microelectrode[29] and tungsten–tungsten oxide film nanoelectrode[30] showed improved stability, fast response time and low impedance towards *in vivo*[24,26] and *in situ* pH measurements.[4,25,27,29,30] The potential (E) of the metal–metal oxide electrode is the result of the equilibrium between the sparingly soluble oxide and its saturated solution and changes according to eqn (1),[25]

$$E = E^0_{M,MO,H^+} - 2.303\frac{RT}{nF}\mathrm{pH} \quad (1)$$

where E^0_{M,MO,H^+} is the standard potential which includes the ionisation product of water and the solubility product of the metal oxide, R is the gas constant (8.314 J mol^{-1} K^{-1}), T is the temperature in Kelvin, F is Faraday's constant (96 485 C mol^{-1}) and n is the number of electrons transferred.

Yamanaka found that the anodic electrodeposition of IrOx films from alkaline iridium oxalate produced smooth, compact, lustrous films. The deposition reaction is given by eqn (2),[31]

$$[Ir(COO)_2(OH)_4]^{2-}(aq) \rightarrow IrO_2(s) + 2CO_2(g) + 2H_2O(l) + 2e^- \quad (2)$$

where the oxidation of the oxalate ligand leads to the liberation of CO_2 and deposition of the hydrated scarcely soluble IrOx. This method has been widely applied for the fabrication of pH sensors from AEIROFs on Au substrates.[25,27,32–36] The anodic electrodeposition of IrOx from iridium oxalate has been carried out using potential cycling,[25,37–40] application of a constant current density,[31,33,41] constant potential[17,27,28] or pulsed potential.[36,40,42]

The reported responses of IrOx electrodes to changes in pH vary considerably in both sensitivity and apparent formal potential ($E^{0\prime}$).[35] To some extent, this depends on the method of preparation – thermally prepared[25,43] and sputtered films[44,45] tend to give varying formal potentials but typically Nernstian responses. IrOx films deposited by anodic potential cycling typically give both varying formal potentials and super-Nernstian responses.[25,46] Hitchman[47] gave an account clearly showing how the variation of $E^{0\prime}$ can arise from varying distributions of Ir(III)/Ir(IV) without necessarily involving changes in sensitivity. Elsewhere[48] he argued that the potential determining reaction for anodically prepared IrOx films is likely to arise from the outer region of the hydrated zone of the oxide film whose composition can be expected to vary according to the precise conditions of deposition. The AEIROFs appear as an intermediate form between the thermal oxide and anodic oxide. The morphology is compact and dense,[27] like the thermal oxide, but super-Nernstian responses are typically achieved. This is due to proton to electron ratios being significantly in excess of 1 due to hydrolysis of a hydrated oxide layer overlying a compact anhydrous oxide.[25,46,48] The general form of the equation is given by,[48]

$$2[IrO_2(OH)_{2-x}(2+x)H_2O]^{(2-x)-}(s) + (3-2x)H^+(aq) + 2e^- \rightleftharpoons [Ir_2O_3(OH)_3\cdot 3H_2O]^{3-}(s) + 3H_2O(l) \quad (3)$$

where x varies according to the degree of film hydration. The varying degrees of hydration depending on the electrodeposition conditions give rise to a super-Nernstian response ranging from −0.061 V per pH to −0.090 V per pH.[35,46] We define a super-Nernstian response as giving at least −0.061 V per pH. This criterion is used since a 5 K error in the reported temperature can cause a Nernstian response of −0.059 V per pH to appear as super-Nernstian with a value of −0.060 V per pH. The super-Nernstian response is desirable as it offers a higher sensitivity to pH measurements, particularly for studies with cells, where the changes in pH might be small. Hence, we chose to use AEIROFs for our pH sensors.

Here we report the use of AEIROF microelectrodes as pH sensors to monitor the acute local pH changes of PAECs in cell culture medium under the stimulation of thrombin. The surface of the chip was coated with air-dried fibronectin for the attachment of PAECs. Fibronectin, an extracellular matrix glycoprotein, has been used for the cell culture of ECs on microelectrode array (MEA) chips[20,21,49] and prevents electrode biofouling with minimal effects on the electrocatalytic properties and active areas of the electrode as shown by our group.[9] Thrombin, a coagulation factor and protease, activates porcine ECs during tissue inflammation[50] and increases energy metabolism in human umbilical vein endothelial cells (HUVECs), leading to extracellular acidification.[51] PD98059, a

MAPK inhibitor, inhibits the action of thrombin and reduces extracellular acidification.[51] Interestingly, the interaction among thrombin, PAECs and fibronectin, and its acute effects on the local extracellular pH have not been studied to date.

Experimental

Chemicals

5 M H_2SO_4 and 85% H_3PO_4 were purchased from Fluka. 37% HCl, 70% HNO_3 and 5 N NH_4OH, KH_2PO_4, iridium(IV) chloride ($IrCl_4$), 50 wt% poly(ethyleneimine) (PEI) (MW ~ 750 000), thrombin from human plasma (T6884), bovine serum albumin (BSA), PD98059, dimethyl sulfoxide (DMSO) and other chemicals used in cell culture were acquired from Sigma-Aldrich. NaOH, KCl and ethanol were obtained from Fisher Scientific. Anhydrous K_2CO_3 was bought from Fisons Scientific Apparatus, oxalic acid dihydrate ($(COOH)_2{\cdot}2H_2O$) and 30% w/w H_2O_2 were from Analar and Decon 90 from Decon Laboratories Limited. Deionised (DI) water with a resistivity of ≥15 MΩ cm from Purite was used to prepare all aqueous solutions.

Instruments

The MEA and its glass chamber, which we collectively termed 'MEA chip', (Fig. 1a), and a chip reader were custom fabricated by Aleria Biodevices as previously reported.[20–22] Each MEA has a Au pseudo-reference electrode (not used), 14 Au working electrodes (25 μm diameter) and a U-shaped Au counter electrode (Fig. 1b). A leak-free, non-porous Ag–AgCl reference electrode (−0.052 V *vs.* saturated calomel electrode (SCE)) (IJ Cambria) was inserted into the glass chamber of the chip through an opening in the chip reader (Fig. 1c). A CHI 1030 electrochemical workstation (CH Instruments, Inc.) was employed to input the experimental parameters and acquire the data. A S20 SevenEasy™ glass pH meter (Mettler Toledo) with temperature display was used to measure the pH of the solutions and the room temperature. Field emission scanning electron microscopy (FESEM) images were captured by a LEO 1525 Gemini. A Leica microscope was used to take the light micrographs.

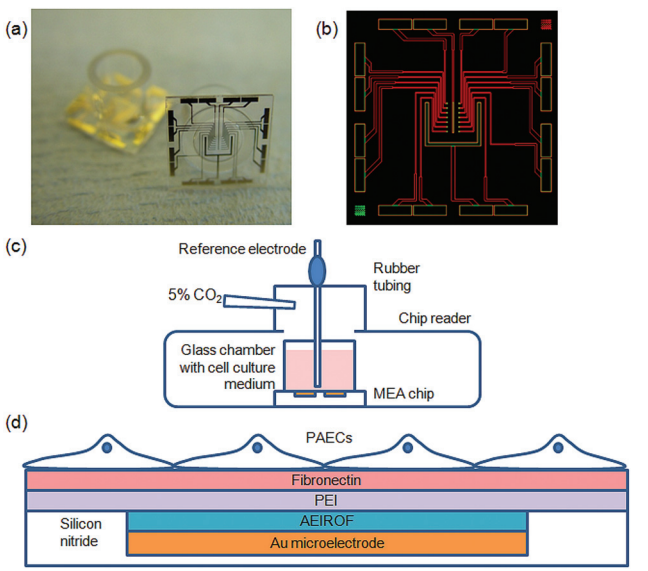

Fig. 1 (a) Photograph of the MEA chip. (b) Mask of MEA with a Au pseudo reference electrode, 14 Au working electrodes (25 μm diameter) and a U-shaped Au counter electrode. (c) Schematic diagram of the side view of the experimental setup for measuring acute local pH changes of PAECs. The MEA chip containing the attached cells in cell culture medium was placed in the chip reader and the setup was gassed with 5% CO_2, 95% air through an oxygen-permeable rubber tubing (sealed at the top) and an external leak-free Ag–AgCl reference electrode was used to measure the open circuit potential. (d) Schematic diagram of the cross section showing a Au microelectrode with AEIROF, which was coated with PEI and fibronectin and then seeded with PAECs.

Preparation of pH sensors on MEA chips

The MEA chips were cleaned sequentially with Decon90, hot DI water, ethanol, 5 M HNO_3 and DI water. The working electrodes, situated in a 1 μm recess, were electrochemically cleaned in 0.5 M H_2SO_4 by CV (−0.5 V to 1.7 V, 0.5 V s^{-1}, 25 cycles) then held at −0.5 V for 5 min to reduce any oxide formed, followed by rinsing with DI water and dried with N_2. AEIROF was electrodeposited by applying a constant current density of 1.70 mA cm^{-2} for 15 min to the iridium oxalate solution, which was prepared according to the method described by Yamanaka.[31] After electrodeposition, the chips were filled with DI water to let the AEIROFs equilibrate overnight. Then, they were dried with N_2 and coated with 20 μL of 5% PEI (optimised) to improve the mechanical stability of the AEIROF, which was otherwise prone to delamination. PEI was chosen over Nafion, which partially redissolved after rehydration and also formed clumps on the silicon nitride surface of the chip, resulting in an uneven coating which would later affect the attachment of PAECs on the chip. PEI was selected over poly(sodium 4-styrenesulfonate) (PSS) and fibronectin as it had the smallest excluded volume among the materials tested (data not shown). The chips were left to dry overnight, then rinsed to remove the excess PEI and filled with DI water and allowed to rehydrate over 1 day.

The chips were then dried with N_2 and coated with 20 μL of 20 μg mL^{-1} fibronectin suspended in Dulbecco's modified Eagle's medium (DMEM) and left to dry overnight in a biological safety cabinet. The excess fibronectin was rinsed off with Dulbecco's phosphate buffered saline (DPBS). The chip could not be coated with fibronectin without the intermediate layer of PEI as the presence of Cl^- in the DMEM reacts with the AEIROF to form a soluble chloroiridate complex[25] and causes the film to dissolve. In addition, fibronectin formed an uneven coating on the silicon nitride surface of the chip.

pH sensor characterisation

Repetitive cyclic voltammetry (CV) was unsuitable for characterising the AEIROFs since the CVs became irreproducible due to the buildup of the poorly conductive Ir(III) oxide with each scan,[38,48] an investigation into which is beyond the scope of this work. Hitchman has shown that variation in $E^{0\prime}$ depends

critically on the potential history which greatly limits the interpretation of the CVs and limits their utility for the characterisation of the oxide film existing prior to voltammetry.[47] We are only interested in the pH range from 4 to 7.7 that is relevant to physiology[52,53] and make no claims for the general utility of our pH sensors. Our previous work showed that the AEIROF sensor does function up to pH 10 or so[27] but this is not relevant to the measurement situation described in this work. Hence, pH calibrations of the PEI-coated AEIROF sensors were performed in chloride-free phosphate buffers of around pH 4.0, 5.0, 6.0, 7.0 and 7.7 made up of 1 M H_3PO_4 and 1 M NaOH at open circuit potential (OCP). The OCP *vs.* time was measured for 5 min in each solution from low to high pH using the CHI 1030. All values of OCP reported here are with respect to the Ag–AgCl reference electrode. The sensitivity is obtained from the slope of the best fit line and $E^{0\prime}$ is given by the pH = 0 intercept, keeping in mind the difficulties of interpreting $E^{0\prime}$ since its value varies even within each type of the IrOx film preparation method as mentioned in the Introduction. The response of AEIROF sensors to changes in the concentration of drugs and other matrix components has been described in our previous studies[27,28] and no interfering effect from DMEM or dissolved O_2 was found.[27]

Cell culture and seeding

PAECs were harvested from freshly excised porcine aortas using collagenase as previously reported.[21] The cells were cultured in a 25 cm^2 tissue culture flask with a cell culture medium containing DMEM supplemented with 1 mg mL^{-1} glucose, 1 mg mL^{-1} sodium bicarbonate, 5 μg mL^{-1} endothelial cell growth factor, 90 μg mL^{-1} heparin, 5 mM L-glutamine, 10% foetal bovine serum, 100 U mL^{-1} penicillin, 100 μg mL^{-1} streptomycin, 2.5 μg mL^{-1} amphotericin and 50 μg mL^{-1} gentamycin at 37 °C and 5% CO_2. PAECs of passage 8 were used for our experiments. These were washed with DPBS, trypsinised and centrifuged at 1000 rpm for 5 min and finally resuspended in the cell culture medium. 30 000 cells in 60 μL of cell culture medium were seeded on one chip to obtain a seeding density of 5×10^5 cells mL^{-1}, while the control chip was filled with 60 μL of the cell culture medium. Both chips were placed in an incubator at 37 °C and 5% CO_2 for 17 h. To prevent evaporation of the cell culture medium, the chips were placed in a large, covered Petri dish along with smaller petri dishes filled with autoclaved DI water.

Addition of reagents for cell experiment

After 17 h, the chip to be tested was removed from the incubator and placed in the chip reader and continuously gassed with 5% CO_2, 95% air (Fig. 1c), for pH control crucial for getting meaningful results. The chip was allowed to reach room temperature and the OCP was recorded for 30 min to obtain the baseline OCP. Reagents were added to the chip at 30 min intervals in the following order – two doses of 5 U mL^{-1} thrombin in 0.1% BSA, then two doses of 50 μM PD98059 in DMSO. This was followed by two additions of 5 μL of 100 mM H_3PO_4 which give the final concentrations of 5.88 mM and 11.11 mM H_3PO_4, respectively, to establish whether the pH sensors were still functioning in the presence of cells at the end of the experiment. There was around a 5 min interval between each addition of reagents as the chip was disconnected from the chip reader and the 5% CO_2 supply and transferred to the biological safety cabinet in an adjacent laboratory for the reagents to be added and for observation under the microscope.

Results and discussion

FESEM characterisation of AEIROF coated with PEI and fibronectin

Fig. 2a shows a FESEM image of the microelectrode after the surface of the chip was coated with 5% PEI, followed by fibronectin (Au–AEIROF–PEI–fibronectin). The PEI coating cannot be observed as the fibronectin coating is thick and forms patches on the silicon nitride surface of the chip. No good images of the PEI-coated AEIROF electrode (Au–AEIROF–PEI) could be obtained as drying the sample during the preparation for FESEM imaging resulted in cracking and delamination of the film.

Fibronectin at high magnification appears as tightly packed clusters with a cobblestone morphology as seen in Fig. 2b. In contrast, PEI on silicon nitride consists of tiny particles which are loosely packed (Fig. 2c). Fibronectin contains the arginine–glycine–aspartic acid (RGD) peptide sequence which promotes EC attachment *via* ligation of integrins found on the surfaces of ECs.[54] The difference in surface morphology in addition to integrin ligation may explain why the PAECS did not attach onto 5% PEI alone but did so in the presence of fibronectin.

Electrochemical characterisation of pH sensors

A super-Nernstian response of −0.066 ± 0.003 V per pH (n = 5) at 22.3 °C is observed for the PEI-coated AEIROFs over the pH range 4.0 to 7.7 in a chloride-free phosphate buffer (Fig. 3). This sensitivity is lower than our group's value of −0.074 V per pH of AEIROF on a Au microelectrode,[27] −0.076 V per pH on a Pt microelectrode[40] and −0.077 V per pH on Pt,[55] but higher than that of −0.059 V per pH on a Pt microelectrode,[34] −0.060 V per pH on a Au thin film[41] and −0.064 V per pH on a Pt macroelectrode.[26] $E^{0\prime}$ is 0.550 ± 0.019 V *vs.* Ag–AgCl or 0.498 V *vs.* SCE at 22.3 °C. This value is lower than 0.732 V *vs.* SCE for AEIROF on a Pt microelectrode.[40] The differences in sensitivity and $E^{0\prime}$ could be due to the electrodeposition method and conditions as mentioned in the Introduction. Nonetheless, the pH sensors showed good reproducibility as the values of the standard deviation in sensitivity and $E^{0\prime}$ represent less than 5% of the respective mean values for 5 electrodes, each prepared on a different chip.

The average 95% response time ($t_{95\%}$) (n = 5) was calculated as the time taken for the sensor to reach ±95% of its OCP at 5 min and found to be 0.3 s for pH 4.0, 19.4 s for pH 5.0, 49.6 s for pH 6.0, 102.4 s for pH 7.0 and 190.2 s for pH 7.7. The increase in response time as pH increases has also been

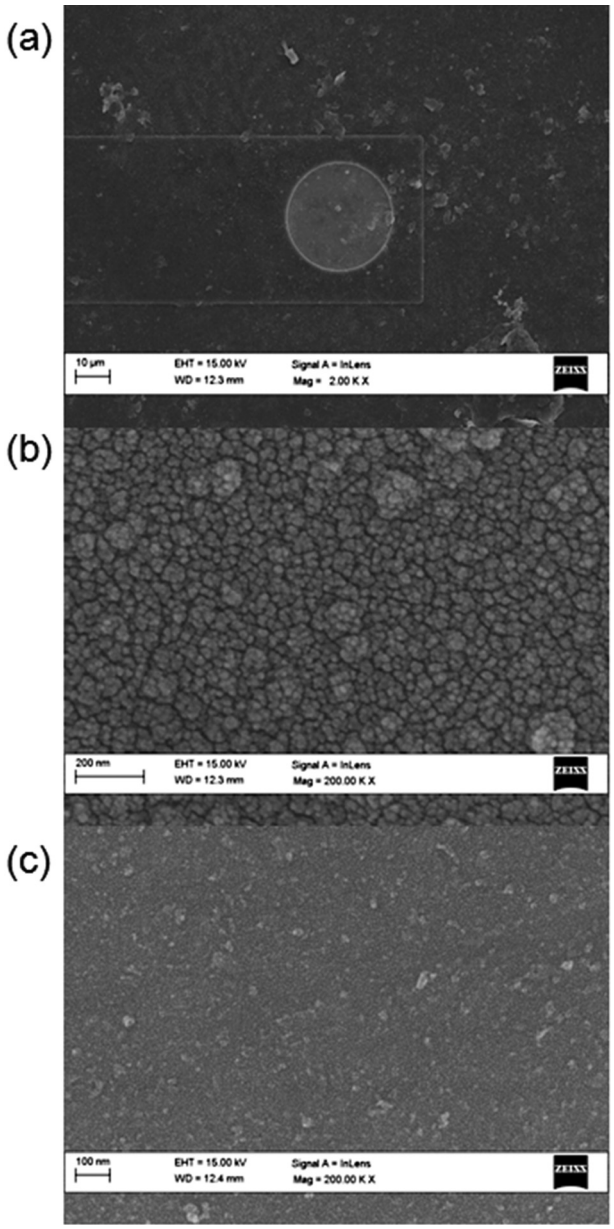

Fig. 2 (a) FESEM image (2000×) of Au–AEIROF–PEI–fibronectin. The central disc is the exposed electrode (25 µm diameter). (b) FESEM image (200 000×) of fibronectin coating on the silicon nitride chip surface. (c) FESEM image (200 000×) of 5% PEI coating on the silicon nitride chip surface.

reported by others.[26,34] It is possible that at lower pH, reduction of Ir(IV) oxide causes the build-up of the poorly conductive Ir(III) oxide,[38,48] resulting in slower charge transfer during the oxidation process at an alkaline pH. A paired two-tailed *t*-test (p = 0.05) showed that there was no significant difference in the sensitivity and $E^{0\prime}$ of the sensors before and after they were coated with fibronectin.

It is important to note that the pH calibration curve and response times obtained here are for the pH measurement of bulk solution, which demonstrates that the sensors are responsive to different pHs. However, the sensors are unable to measure the actual value of the local pH in the immediate environment of the cells because the local pH is different from the pH of the bulk solution due to the heterogeneous nature of release of H^+, lactate, CO_2 and other products from the cells which can affect the local extracellular pH. It is therefore more meaningful to use the sensors to track whether the local pH of the cells increases or decreases based on a decrease and increase in OCP, respectively. An estimated change in local pH can then be calculated based on the sensitivity of the sensor.

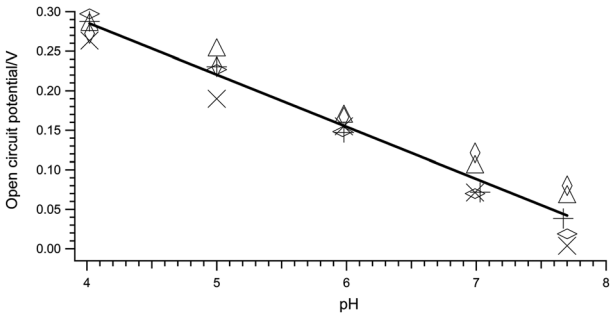

Fig. 3 Plot of open circuit potential/V against pH for Au–AEIROF–PEI from pH 4.0 to 7.7 in chloride-free phosphate buffer at 22.3 °C. Each type of marker represents a PEI-coated AEIROF electrode on a different chip.

Real-time measurement of local pH changes of control chip

The data acquired for the control experiment (dotted lines) and PAEC experiment (solid lines) are presented in Fig. 4. Curve smoothing was carried out using a Savitzky–Golay filter with second order polynomial fitting with 301 points (30.1 s) for each of the 30 min runs. The increase in OCP with respect to the baseline OCP caused by the addition of each reagent was obtained by subtracting the OCP recorded for the reagent by the baseline OCP. This value was divided by the sensitivity

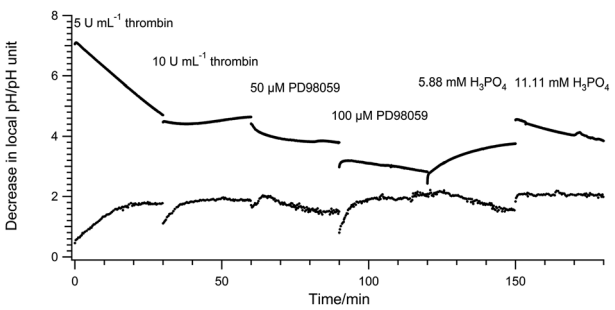

Fig. 4 Decrease in local pH/pH unit (with respect to the baseline pH) against time/min for the control experiment (dotted lines) and the experiment with PAECs (solid lines). The reagents were added in the order of 5 U mL^{-1} thrombin, 10 U mL^{-1} thrombin, 50 µM PD98059, 100 µM PD98059, 5.88 mM H_3PO_4 and 11.11 mM H_3PO_4 at 0 min, 30 min, 60 min, 90 min, 120 min and 150 min, respectively. The experiments were performed at an average room temperature of 22.0 °C and gassed with 5% CO_2, 95% air.

of the sensor to obtain an estimated decrease in local pH for each reagent over time.

The addition of 5 U mL^{-1} human plasma thrombin to the control chip induced a local decrease of 1.71 pH units at 30 min, likely due to the dissolution of fibronectin by thrombin. Galdal *et al.* reported that 2 NIH U mL^{-1} bovine thrombin induced the loss of extracellular fibronectin fibrils from HUVECs in 30 min.[56] Furthermore, when the control chip was seeded with PAECs at the end of the experiment, the PAECs failed to attach and appeared round, suggesting that the fibronectin had been denatured or lost during the control experiment. A second dose of thrombin did not appear to have an appreciable effect on changing the local pH.

The first dose of PD98059 increased the local pH by 0.36 pH unit at 30 min compared to the second dose of thrombin while the second dose of PD98059 decreased the local pH by 0.53 pH unit at 30 min compared to the first dose of PD98059. Nonetheless, any effect of the reagents on the local pH could be offset by measuring the changes in pH for the cell experiments with respect to the control experiment for the addition of the corresponding reagent.

The concentrations of the H_3PO_4 added after the two doses of PD98059 were carefully chosen to be within the buffer capacity of the cell culture medium and also to prevent further denaturation of fibronectin. The addition of the acid would demonstrate that had the buffer capacity of the cell culture medium been exceeded due to the action of the reagents, an obvious decrease in the local pH should be recorded if the pH sensor was still functioning. The addition of 5.88 mM H_3PO_4 caused the local pH to increase by 0.49 pH unit compared to the second dose of PD98059. This could be due to the H^+ combining with the HCO_3^- in the cell culture medium to form H_2CO_3 and CO_2 and hence adding to the buffer capacity of the solution. The local pH was stable upon giving 11.11 mM H_3PO_4, indicating that the $HCO_3^-/H_2CO_3/CO_2$ equilibrium had been re-established.

Real-time measurement of local pH changes of PAECs

Plainly visible blue IrOx was observable in light micrographs (data not shown) taken before and after exposure to cells. Fig. 5a confirms that the PAECs were healthy with their characteristic stretched, polygonal morphology at sub-confluent levels. From Fig. 4, it can be seen that the first dose of thrombin initially caused a sharp decrease of 7.05 pH units which reduced to 4.70 pH units by the end of 30 min. This indicates that thrombin induced rapid extracellular acidification of PAECs as expected, likely due to increased glycolysis and Na^+/H^+ exchange by the cells.[51] This indicates an increase in cell metabolism, causing an acute decrease in local pH. Since a decrease of 1.71 pH units can be attributed to the dissolution of fibronectin, the decrease of 2.99 pH units at 30 min is due to the effect of 5 U mL^{-1} thrombin on the PAECs. The reduction in the decrease of local pH over 30 min may be attributed to two factors. First, H^+ produced by the PAECs around the sensor diffused into the bulk solution due to natural convection, thereby reducing the concentration of H^+ around the sensor. Second, there was a reduction in extracellular acidification as the PAEC morphology changed from a polygonal phenotype (Fig. 5a) to a contracted phenotype by the end of 30 min, which may be attributed to the loss of fibronectin.[56] This caused the PAECs to lose their anchorage and become round. Such a change in cell shape was reported by Galdal *et al.* after exposing confluent monolayer cultures of HUVECs to 0.5 NIH U mL^{-1} human α-thrombin for 30 min, which made the cell membrane more permeable,[57] likely due to the rapid disassembly of claudin-5 from the tight junctions of the cells.[58]

The second dose of thrombin elicited a stable local pH and had a net effect of decreasing the local pH by 2.77 pH units compared to the control. The pH was stable for the second dose of thrombin compared to the first probably because the rate of change of PAECs from the polygonal phenotype to the contracted phenotype had reached its maximum, so the rate of cell metabolism was quite stable.

Despite the loss of fibronectin, the pH sensors could still respond to pH changes. The addition of 50 μM PD98059 caused the local pH to decrease by 2.29 pH units compared to the control, which is 0.48 pH unit lesser than the second dose of thrombin. This means that the pH had increased compared to the second dose of thrombin, which indicates a reduction in extracellular acidification due to PD98059 as expected.[51] This is because PD98059 inhibited MAPK and hence the intracellular pathway through which thrombin acts,[59] thereby leading to a decrease in cell metabolism.

The local pH decreased by 0.78 pH unit compared to the control for the second dose of PD98059. This value is 1.51 pH units lesser than the 50 μM PD98059, which shows that 100 μM PD98059 further reduced extracellular acidification. However, PD98059 did not cause the cells to recover their polygonal phenotype (Fig. 5b).

When 5.88 mM H_3PO_4 was added, a gradual decrease in the local pH was observed and the pH was lower than that of the control by 2.20 pH units after 30 min. This value is larger than that of 100 μM PD98059 by 1.42 pH units. Further addition of H_3PO_4 to a final concentration of 11.11 mM induced a decrease in pH by 1.84 pH units after 30 min, which is larger than that of 5.88 mM H_3PO_4 by 0.42 pH unit. This shows that

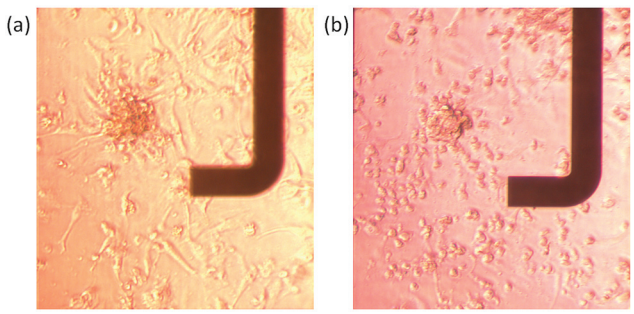

Fig. 5 Light micrographs (100×) of PAECs on a chip (a) after removing from the incubator and (b) after the second dose of PD98059.

the pH sensor is still functioning and the buffer capacity of the cell culture medium had been depleted by the previous steps, so the addition of acid caused the pH to decrease.

Conclusion

We are in the early days of developing systems that allow for the characterisation of acute cellular responses. In this work, we used an AEIROF microsensor to monitor and estimate the decrease in local pH of PAECs attached on the fibronectin-coated sensor in response to thrombin. The local pH of the cells decreased sharply in the presence of thrombin. Thrombin induced the dissolution of fibronectin and the PAECs exhibited a change in cell morphology as they lost their attachment to fibronectin. We probed the intracellular pathway responsible for the action of thrombin on the PAECs by adding the MAPK inhibitor, PD98059, and monitoring the change in local pH of the cells on the pH microsensor. The local pH increased when PD98059 was added, which reflects a decrease in cell metabolism as MAPK was inhibited. This confirms that the intracellular pathway for the action of thrombin on PAECs is dependent on MAPK. Taken together, the results provide us some insights into the biological interaction of thrombin, PAECs and fibronectin. Thrombin activated PAECs by causing them to detach from the extracellular matrix and increased their metabolism and caused cytoskeleton reorganisation, likely in preparation for proliferation and migration as observed in thrombin-mediated angiogenesis.[51] Overall, this study demonstrates that our AEIROF microelectrodes are useful for tracking local pH changes of cells on the sensors to investigate their metabolic responses to a stimulus in real-time. In addition, it allows us to identify the intracellular pathway through which the stimulus exerts its effects on the cells. Our pH microsensors are highly promising for gaining insights into the real-time interaction of cells, soluble factors and the extracellular matrix.

Acknowledgements

Shu Rui Ng is grateful to the Nanyang Technological University for a Ph.D. scholarship. The authors are grateful to Medermica Ltd for financial support.

References

1 A. S. Johnson, A. Selimovic and R. S. Martin, *Anal. Bioanal. Chem.*, 2013, **405**, 3013–3020.
2 J. Wang, C. Wu, N. Hu, J. Zhou, L. Du and P. Wang, *Biosensors*, 2012, **2**, 127–170.
3 L. Ding, D. Du, X. Zhang and H. Ju, *Curr. Med. Chem.*, 2008, **15**, 3160–3170.
4 I. A. Ges, B. L. Ivanov, A. A. Werdich and F. J. Baudenbacher, *Biosens. Bioelectron.*, 2007, **22**, 1303–1310.
5 T. Haruyama, *Adv. Drug Delivery Rev.*, 2003, **55**, 393–401.
6 K. Sato, Y. Tanaka, B. Renberg and T. Kitamori, *Anal. Bioanal. Chem.*, 2009, **393**, 23–29.
7 C. X. Guo, S. R. Ng, S. Y. Khoo, X. Zheng, P. Chen and C. M. Li, *ACS Nano*, 2012, **6**, 6944–6951.
8 J. El-Ali, P. K. Sorger and K. F. Jensen, *Nature*, 2006, **442**, 403–411.
9 R. Trouillon, Z. Combs, B. A. Patel and D. O'Hare, *Electrochem. Commun.*, 2009, **11**, 1409–1413.
10 T. N. Sato and S. Loughna, in *Mouse Development: Patterning, Morphogenesis, and Organogenesis*, ed. J. Rossant and P. P. L. Tam, Academic Press, Canada, 2002, pp. 211–233.
11 J. Goveia, P. Stapor and P. Carmeliet, *EMBO Mol. Med.*, 2014, **6**, 1105–1120.
12 P. Fraisl, M. Mazzone, T. Schmidt and P. Carmeliet, *Dev. Cell*, 2009, **16**, 167–179.
13 E. Gee, M. Milkiewicz and T. L. Haas, *J. Cell Physiol.*, 2010, **222**, 120–126.
14 J. C. Owicki and J. W. Parce, *Biosens. Bioelectron.*, 1992, **7**, 255–272.
15 S. Mohri, J. Shimizu, N. Goda, T. Miyasaka, A. Fujita, M. Nakamura and F. Kajiya, *Sens. Actuators, B*, 2006, **115**, 519–525.
16 D. O'Hare, in *Body Sensor Networks*, ed. G.-Z. Yang, Springer-Verlag, London, 2nd edn, 2014, pp. 55–115.
17 D. O. Wipf, F. Ge, T. W. Spaine and J. E. Baur, *Anal. Chem.*, 2000, **72**, 4921–4927.
18 C. Kranz, A. Kueng and B. Mizaikoff, Sensors, 2004. Proceedings of IEEE, 2004.
19 B. P. Nadappuram, K. McKelvey, R. Al Botros, A. W. Colburn and P. R. Unwin, *Anal. Chem.*, 2013, **85**, 8070–8074.
20 R. Trouillon, D.-K. Kang, H. Park, S.-I. Chang and D. O'Hare, *Biochemistry*, 2010, **49**, 3282–3288.
21 R. Trouillon, C. Cheung, B. A. Patel and D. O'Hare, *Biochim. Biophys. Acta, Gen. Subj.*, 2010, **1800**, 929–936.
22 R. Trouillon, E. D. Williamson, R. J. Saint and D. O'Hare, *Biosens. Bioelectron.*, 2012, **38**, 138–144.
23 N. W. Carter, F. C. Rector Jr., D. S. Campion and D. W. Seldin, *J. Clin. Invest.*, 1967, **46**, 920–933.
24 H. W. Haggard and L. A. Greenberg, *Science*, 1941, **93**, 479–480.
25 D. O'Hare, K. H. Parker and C. P. Winlove, *Med. Eng. Phys.*, 2006, **28**, 982–988.
26 S. A. M. Marzouk, S. Ufer, R. P. Buck, T. A. Johnson, L. A. Dunlap and W. E. Cascio, *Anal. Chem.*, 1998, **70**, 5054–5061.
27 E. Bitziou, D. O'Hare and B. A. Patel, *Anal. Chem.*, 2008, **80**, 8733–8740.
28 E. Bitziou, D. O'Hare and B. A. Patel, *Analyst*, 2010, **135**, 482–487.
29 Y. Ha, D. Myung, J. H. Shim, M. H. Kim and Y. Lee, *Analyst*, 2013, **138**, 5258–5264.
30 K. Yamamoto, G. Shi, T. Zhou, F. Xu, M. Zhu, M. Liu, T. Kato, J.-Y. Jin and L. Jin, *Anal. Chim. Acta*, 2003, **480**, 109–117.
31 K. Yamanaka, *Jpn. J. Appl. Phys., Part 1*, 1989, **28**, 632–637.

32 K. Pasztor, A. Sekiguchi, N. Shimo, N. Kitamura and H. Masuhara, *Sens. Actuators, B*, 1993, **12**, 225–230.
33 S. C. Mailley, M. Hyland, P. Mailley, J. M. McLaughlin and E. T. McAdams, *Mater. Sci. Eng., C*, 2002, **21**, 167–175.
34 A. N. Bezbaruah and T. C. Zhang, *Anal. Chem.*, 2002, **74**, 5726–5733.
35 H. A. Elsen, C. F. Monson and M. Majda, *J. Electrochem. Soc.*, 2009, **156**, F1–F6.
36 S. Carroll and R. P. Baldwin, *Anal. Chem.*, 2010, **82**, 878–885.
37 J. Mozota and B. E. Conway, *Electrochim. Acta*, 1983, **28**, 1–8.
38 L. D. Burke and D. P. Whelan, *J. Electroanal. Chem. Interf. Electrochem.*, 1984, **162**, 121–141.
39 M. L. Hitchman and S. Ramanathan, *Analyst*, 1988, **113**, 35–39.
40 Y. Lu, T. Wang, Z. Cai, Y. Cao, H. Yang and Y. Y. Duan, *Sens. Actuators, B*, 2009, **137**, 334–339.
41 T. Y. Kim and S. Yang, *Sens. Actuators, B*, 2014, **196**, 31–38.
42 W. Olthuis, M. A. M. Robben, P. Bergveld, M. Bos and W. E. van der Linden, *Sens. Actuators, B*, 1990, **2**, 247–256.
43 S. Ardizzone, A. Carugati and S. Trasatti, *J. Electroanal. Chem. Interf. Electrochem.*, 1981, **126**, 287–292.
44 T. Katsube, I. Lauks and J. N. Zemel, *Sens. Actuators*, 1981, **2**, 399–410.
45 S. F. Cogan, J. Ehrlich, T. D. Plante, A. Smirnov, D. B. Shire, M. Gingerich and J. F. Rizzo, *J. Biomed. Mater. Res., Part B*, 2009, **89B**, 353–361.
46 L. D. Burke, J. K. Mulcahy and D. P. Whelan, *J. Electroanal. Chem. Interf. Electrochem.*, 1984, **163**, 117–128.
47 M. L. Hitchman and S. Ramanathan, *Talanta*, 1992, **39**, 137–144.
48 M. L. Hitchman and S. Ramanathan, *Electroanalysis*, 1992, **4**, 291–297.
49 R. Trouillon, D. O'Hare and S. I. Chang, *Biochem. Mol. Biol. Rep.*, 2011, **44**, 699–704.
50 D. Chen, K. Riesbeck, J. H. McVey, G. Kemball-Cook, E. G. D. Tuddenham, R. I. Lechler and A. Dorling, *Xenotransplantation*, 2001, **8**, 258–265.
51 Y. Fan, D.-Z. Wu, Y.-Q. Gong, R. Xu and Z.-B. Hu, *Biochem. Biophys. Res. Commun.*, 2002, **293**, 979–985.
52 W. F. Ganong, *Review of Medical Physiology*, McGraw-Hill Companies, New York, 22nd edn, 2005, pp. 729–738.
53 A. C. Guyton and J. E. Hall, *Textbook of Medical Physiology*, Elsevier Saunders, Philadelphia, 11th edn, 2006, pp. 383–401.
54 S. Kim, K. Bell, S. A. Mousa and J. A. Varner, *Am. J. Pathol.*, 2000, **156**, 1345–1362.
55 V. M. Tolosa, K. M. Wassum, N. T. Maidment and H. G. Monbouquette, *Biosens. Bioelectron.*, 2013, **42**, 256–260.
56 K. S. Galdal, S. A. Evensen and E. Nilsen, *Thromb. Res.*, 1985, **37**, 583–593.
57 K. S. Galdal and S. A. Evensen, *Thromb. Res.*, 1981, **21**, 273–284.
58 N. Kondo, M. Ogawa, H. Wada and S.-I. Nishikawa, *Exp. Cell Res.*, 2009, **315**, 2879–2887.
59 N. E. Tsopanoglou and M. E. Maragoudakis, *J. Biol. Chem.*, 1999, **274**, 23969–23976.